



OPEN

# Energy efficient traffic data aggregation and routing for metropolitan optical access network

T. Senthil Kumar<sup>1</sup>✉, Mohan. V<sup>2</sup> & S. Senthilkumar<sup>3</sup>

The Energy Efficient Regional Area Metropolitan Optical Access Network (MOAN) is a modern optical communication system specifically designed for metropolitan areas. It addresses the increasing demand for high-speed data transmission while optimizing energy consumption. In this paper, energy-efficient traffic data aggregation and energy-aware routing are presented to increase the network lifetime of the system. The traffic data aggregation reduces redundant transmissions, while energy-aware routing minimizes energy consumption by selecting energy-efficient paths. Initially, the wavelength utility-based dynamic wavelength allocation approach (WU-DWA) was developed to facilitate efficient resource utilization. Then, the data aggregation is performed in the context of traffic grooming using the adaptive principal component analysis (APCA) technique. APCA combines or grooms multiple low-bandwidth data streams into higher-capacity data channels to optimize the use of available network resources, such as wavelengths in optical networks or channels in general communication systems. The aggregated data is routed with the proposed energy efficient adaptive Tuna slap Swarm Optimization strategy (ATSSO). By using the proposed approach, the performance obtained in terms of energy consumption is 88, throughput is 131.63, average packet delay is 3.551, and energy savings are 29.99, respectively. The proposed approach is implemented, and the performance is evaluated in terms of standard performance metrics and analyzed using traditional approaches. The better performance indicates that the proposed approach is more efficient than existing approaches.

**Keywords** Metropolitan optical access network, Energy efficient routing, Dynamic wavelength allocation, Traffic data aggregation

## Abbreviations

$\delta_m$	Traffic proportion
$E_a$	Bandwidth request with best effort
$A_a$	Bandwidth request with assured forwarding
$B_a$	Bandwidth request with expedited forwarding
$H$	Wavelength capacity
$\varepsilon_k$	Number of wavelengths allocated to VPON
$D_{over,m}$	Excess bandwidth
$G$	Number of VPON
$\chi$	Constraint parameter
$T_{BW}$	Total VPON capacity
$T_L$	Total requested bandwidth
$D_{B,temporary}^a$	Temporary bandwidth allocated for best effort
$D_{A,temporary}^a$	Temporary bandwidth allocated for assured forwarding
$D_{E,temporary}^a$	Temporary bandwidth allocated for expedited forwarding
$L_B^a$	Bandwidth of best effort

<sup>1</sup>Department of Electronics and Communication Engineering, M.Kumarasamy College of Engineering, Karur, Tamilnadu 639113, India. <sup>2</sup>Department of Electrical and Electronics Engineering, E.G.S. Pillay Engineering College, Nagapattinam, Tamilnadu 611002, India. <sup>3</sup>Department of Electronics and Communication Engineering, E.G.S. Pillay Engineering College, Nagapattinam, Tamilnadu 611002, India. ✉email: tskumar5585@gmail.com

$L_A^a$	Bandwidth of assured forwarding
$L_E^a$	Bandwidth of expedited forwarding
$D_{B,pre}^a$	Predicted bandwidth for best effort
$D_{A,pre}^a$	Predicted bandwidth for assured forwarding
$D_{E,pre}^a$	Predicted bandwidth for expedited forwarding
$Y$	Input data
$p \times i$	Step size
$Y_j$	Feature size
$\mu_q$	Initial eigenvalues
$\Omega$	Orthogonal projection matrix
$A$	Projection data
$En$	Energy consumption
$NL$	Network lifetime
$PR$	Packet delivery ratio
$Dy$	Delay
$x_1, x_2, x_3$ , and $x_4$	Normalization factors
$rand$	A random number between [0, 1]
$UB$	Upper bound
$LB$	Lower bound in the search space.
$TP$	Total population
$q_j^u$	Initialization of the tuna population
$Y_{u+1}^j$	Position of the individual in $u + 1$ iteration
$Y_{bst}^u$	The optimal position of the current individual
$Y_{rnd}^u$	Randomly generated position based on the individual in the search space
$\beta_1, \beta_2$	Weight coefficients for controlling the movement towards optimal individuals.
$d$	Degree of coefficient
$u$	Number of iterations
$u_{max}$	Maximum number of iterations
$m$ and $\gamma$	Intermediate variables
$c$	Random number.
$T_F$	Random number between -1 and 1 for controlling the population of direction.
$q$	Adjustment factor
$M$	Total number of iterations
$m$	Current iteration
$d_2$ and $d_3$	Random numbers

With the rapid growth of communication traffic, data centric applications are used in wide area networks (WANs). Artificial intelligence (AI) and Machine Learning (ML) applications are being utilized for communication between data centers and users in the fields of science, business, entertainment, and social networking<sup>1</sup>. Optical access networks (OAN) are used as a major solution for broadband access across the world. Metropolitan access network (MAN) ensures higher bandwidth and data rate to meet the requirements in the past decades<sup>2</sup>. In next generation optical networks, MOAN is the solution for low operating cost, low latency, big capacity, and high transmission efficiency<sup>3</sup>. Passive Optical Network (PON) employs the optical line terminal (OLT) at the center to maintain the data transmission to the users. OLT is followed by Optical Network Units (ONU), which coordinate the user data transmissions<sup>4</sup>. A passive optical splitter is deployed between OLT and ONUs. Most of the PON systems are based on time division multiplexing (TDM) technology<sup>5</sup>. Furthermore, a group of photonic wireless technologies, including free space optical (FSO), optical camera communication (OCC), Light Fidelity (LiFi), and Visible Light Communication (VLC), are used for connecting the end user<sup>6,7</sup>.

The mobile network research group has been thinking about new ways of communicating, such as THz/mm Wave channels, to meet the growing need for bandwidth<sup>8</sup>. Also, the traditional data center architecture model focused on several challenges, including reliability, scalability, and efficient communication<sup>9</sup>. However, the rapid utilization of optical systems requires energy efficient and scalable modeling. When increasing the data rate and the number of users, the power consumption and energy efficiency are mainly focused on<sup>10</sup>. The solutions are provided in terms of sleep mode activation, converting the network components with low load, etc<sup>11</sup>. By integrating the power scheduling approaches with finer backhaul and frontend, dynamic adaptive strategies are being utilized<sup>12</sup>. These strategies adapt the power state of ONU based on the traffic profile and User equipment (UE) connection constraints. To achieve the tradeoff between the latency and power consumption, the weighted objective function is utilized<sup>13</sup>. Furthermore, high coherence between each frequency is challenged and limited by the capacity and effectiveness of these approaches<sup>14</sup>.

With a transmission speed of up to 40 Gbit/s, OMAN was built to accommodate the increasing need for bandwidth<sup>15</sup>. Improving spectral efficiency is achieved through the use of multilevel communication protocols. Using dynamic bandwidth allocation (DBA), a new PON standard was designed to maximize the use of the existing architecture<sup>16</sup>. In this framework, algorithms are developed to share the resources based on the advantages of carrier availability. The network performance can be improved with a data aggregation procedure<sup>17</sup>. This process integrates several data packets into a single one before transmission<sup>18</sup>. These aggregation networks use gateways for data packet forwarding between the core network and the access network. It integrates the data from access networks and forwards it to the service gateway. The service gateway serves as an interface between the core and the aggregation network<sup>19</sup>. The routing approaches involve effective data forwarding towards optimal performance. Nodes involved in the network decide the routing techniques based on the requirement<sup>20</sup>. Several

routing techniques have been suggested in recent years for optimal performance. However, energy efficiency is still considered a challenging issue due to the dynamic nature of the environment.

However, while optical access networks (OANs) and advanced PON standards have improved bandwidth and cost-efficiency, they often face challenges with real-time adaptability and energy optimization, especially under dynamic load conditions. Although techniques like sleep mode operation and dynamic power allocation reduce power consumption, they may introduce added latency and complexity in coordination. Similarly, while MOAN improves spectral efficiency, the need for complex multilevel protocols and accurate traffic forecasting can limit its practical scalability. Moreover, current routing and aggregation strategies enhance throughput and reduce redundancy but often lack responsiveness to real-time user behavior or application-specific latency constraints. Therefore, a tradeoff exists between network performance, energy efficiency, and architectural complexity that remains unresolved in current models.

In next-generation networks, there is a need for scalable, energy-efficient, and low-latency communication infrastructures due to data demands and energy consumption. Although recent advancements in PON-based architectures, OWC integration, and optimization models have contributed to performance improvements, many existing solutions are limited by static resource allocation, infrastructure complexity, and insufficient adaptability to dynamic user and traffic requirements. Furthermore, emerging applications such as machine learning, federated learning, and real-time services require flexible and intelligent network management strategies that can operate efficiently under diverse conditions. These gaps motivate the need for a novel, adaptive, and cost-effective PON-based architecture that leverages intelligent control mechanisms to meet the growing demands for high bandwidth, low power consumption, and reliable communication in future data centers and access networks.

Some strategies use other strategies to optimize performance, while others are based on the goal of dispersing requests over the network<sup>21,22</sup>. At the same time, the DBA includes the utilization of more channels enabled with wavelength division multiplexing (WDM). However, the PON performance is affected by dynamic traffic, diversity, and increased data volume. Time- and wavelength-dependent PONs have distinct wavelength properties. The efficiency of PON is impacted by various issues, such as the loss of resources and delays. An energy-efficient approach is necessary to improve the network lifetime and guarantee improved performance, which is mostly concerned with routing techniques. Therefore, in order to make the most of cutting-edge technology, algorithms like optimal routing, dynamic wavelength allocation, and bandwidth allocation need to be developed.

By considering the above-mentioned factors, the contribution of the proposed work is described below.

- To develop an energy efficient Virtual passive access network (VPON) architecture with better communication performance in terms of energy efficiency, delay, and throughput.
- To ensure efficient usage of network capacity and optimize the data transmission through wavelength allocation and bandwidth allocation procedures.
- To integrate the lower bandwidth stream into a higher bandwidth stream through a data aggregation procedure, enhanced the bandwidth efficiency with less overhead.
- To route the aggregated traffic through the network to achieve minimal energy consumption while ensuring good performance.
- To develop an energy-efficient routing approach using an optimization algorithm that improves energy consumption, network lifetime, and throughput by detecting the optimal forwarder node.

The paper organization is given as follows. Recent approaches related to energy efficient OAN were given in Sect. [Related work](#). A detailed description of the proposed methodology is given in Sect. [Proposed methodology](#). The experimental analysis and discussion are given in Sect. [Experimental evaluation](#), and the conclusion is given in Sect. [Conclusion](#).

## Related work

The recent research related to the proposed approach is given below.

Abrar S. Alhazmi et al.<sup>23</sup> integrated PON and Optical wireless communication (OWC) into next generation spine-and-leaf (SL) Data Centre Networks (DCNs). OWC systems are used to connect the data centers through a WDM Infrared (IR) transceiver. In distributed access points (AP), the transceivers were placed. Moreover, each transceiver is connected through a leaf switch to connect to the server within the track. In this configuration, the spine switches are replaced with Network Interface Cards (NIC) and OLT to achieve better connectivity. OWC-PON-based SL DC has reduced the power consumption by 46% while considering eight tracks.

Wafaa B. M. Fadlelmula et al.<sup>24</sup> developed energy efficient PON model for backhaul connectivity in indoor VLC systems. It permits the user to process demand for accessing different fog and processing devices of the end user in the same buildings. Fog resources complement fog nodes at the metro, access network and central cloud data center. In order to improve energy efficiency with the user needs, a Mixed Integer Linear Programming (MILP) approach is introduced. The analysis was performed between the serving and allocating demand in a conventional cloud data center. Furthermore, the proposed architecture is analyzed in relation to the connectivity of SL. Based on the SL architecture and serving demand, the PON base architecture has achieved power reduction of 86% and 84%, respectively.

Recent advancements have used AI approaches for machine-to-machine (M2M) communication. This requires the development of sophisticated functionalities in advanced PON. Andrew Fernando Pakpahan et al.<sup>25</sup> introduced software-defined architecture for Time- and Wavelength-Division Multiplexed (TWDM)-PON, which is modeled to support the traffic of federated learning (FL) in a peer-to-peer (P2P) manner. This architecture combines the P2P-FL-ONU, P2P-FL-DBA, and advanced P2P-FL-OLT with dedicated P2P-FL-

DBA. It can also manage the traffic by improving the system throughput in terms of packet loss ratio, jitter, and delay.

PON is an effective methodology for enabling fiber-to-the-home networks. When compared with digital subscriber loops (DSL), power consumption is minimized for a significant portion of a telecommunication network. Several types of research, including the modelling of next generation power efficient PON, sleep mode, optimal PON dimensioning, wavelength split time, TWDM-PON, wavelength-switched TWDM-PON, and bit-interleaved PON (Bi-PON), were developed in recent years. In order to minimize power consumption, Sukriti Garg and Abhishek Dixit<sup>26</sup> developed analytical modeling in which the optimal grade of service to the user is achieved to show the sleep mode functionality. Moreover, hybrid sleep mode aware techniques and dynamic allocation techniques have been developed with less access power efficiency.

Mohammed Alharthi et al.<sup>27</sup> presented the architecture of a two-tier arrayed waveguide grating router (AWGR)-based PON data center to improve the performance. It considers several scenarios of link failure to analyze the resilience of modelling. For optimizing the data traffic over several failure scenarios, the MILP model is developed in which delay and power consumption are reduced by 10% and 61%, respectively.

The service-based techniques are utilized for optimizing latency, reliability, and network utilization. Giap Le et al.<sup>28</sup> developed a reliable provisioning technique for optimal data center selection over several disjoint paths. The integer linear programming is formulated with the development of heuristic approaches and resolved using realistic network instances. This approach has improved the utilization of network resources, and it is suitable for reliable communication.

Soheil Hosseini et al.<sup>29</sup> developed dynamic multipath routing with modulation level, spatial and spectrum allocation approaches. Space division multiplexing (SDM) assisted elastic optical networks (EON), which had been utilized with bandwidth variable transponders (BVTs) for a multipath routing strategy. Moreover, the utilization of multi-core fibers (MCFs) is eliminated due to inter-core crosstalk (XT), and it minimizes the quality of the received signal. Hence, the modulation format ensures that the XT of the light path does not exceed the threshold for each modulation format.

Yunwu Wang et al.<sup>30</sup> developed OTNs with physical layer security, which is differentiated from traditional optical networks. After that, the 5G RAN slice mapping issue in the physical layer secured MA-EON is formulated as an integer linear programming (ILP) model for reducing average cost. In the ILP model, the non-scalability issue is resolved using heuristic-assisted deep reinforcement learning (HA-DRL) that assures optimal solutions in large scale networking. The shortest path approach reduces the size of the exploration space and accelerates the convergence process.

The comparison of existing approaches is given in Table 1.

The existing approaches demonstrate the development of integrated PON with different technologies to improve scalability, reliability, and energy efficiency in data center and communication networks. Approaches such as OWC-PON hybrid architectures, software-defined TWDM-PON for federated learning, energy-efficient VLC backhaul systems, and AWGR-based PON architectures have shown considerable power savings and performance improvements. Optimization methods, including MILP and heuristic algorithms, have been widely applied to reduce power consumption, delay, and enhance network resource utilization. However, the existing works largely focus on static or specific network scenarios with limited adaptability to dynamic user demands or real-time traffic scenarios. Moreover, many solutions rely on complex infrastructure (e.g., SDM-EON, multi-tier PONs), which can increase deployment cost and complexity. There is also a gap in integrating machine learning-based dynamic resource management into energy-aware PON systems to address scalability and latency under real-time traffic loads. These limitations are considered open research issues for developing more adaptive, intelligent, and cost-efficient architectures.

Techniques	Objectives	Advantages	Disadvantages
OWC-PON-based SL DC (Abrar S. Alhazmi et al. <sup>21</sup> )	To achieve better connectivity and to minimize the power consumption.	Power consumption is minimized.	The effect of OEC is not considered for workload placement.
MILP, SL (Wafaa B. M. Fadlelmula et al. <sup>22</sup> )	To provide backhaul connectivity and minimize power consumption.	Optimal allocation is achieved with low power consumption.	The modelling is not evaluated with different configuration scenarios.
Advanced P2P-FL-OLT architecture (Andrew Fernando Pakpahan et al. <sup>23</sup> )	To improve the efficiency of PON system performance with a decentralized P2PFL communication system.	Reliable and low latency communication was achieved.	This approach is not suitable for real-time simulation scenarios.
TWDM-PON, dynamic allocation technique, Bi-PON (Sukriti Garg and Abhishek Dixit <sup>24</sup> )	To evaluate power saving with optimal PON dimensioning.	Higher accuracy can be achieved.	This approach is not applicable to more realistic scenarios.
AWGR-based PON, MILP (Mohammed Alharthi et al. [25])	To optimize traffic routing under various scenarios.	Power consumption and delay are minimized.	The complexity of the model architecture was not evaluated.
Reliable service provisioning (Giap Le et al. <sup>28</sup> )	To optimize the capacity of each link.	Improved reliability and reduced latency.	The real-time scenario is not evaluated.
Dynamic multipath routing (Soheil Hosseini et al. <sup>29</sup> )	To minimize the blocking probability and energy consumption.	Low energy consumption and low latency.	This approach is not suitable for real-time scenarios.
heuristic-assisted DRL (Yunwu Wang et al. <sup>30</sup> )	To resolve latency and security requirements.	Higher resource efficiency can be achieved.	The complexity of the approach is not considered.

**Table 1.** Comparison of existing approaches.

## Proposed methodology

The performance of the access network can be improved with the integration of PON and virtualization. It develops a logical level network modelling, and it is flexible for real-time modeling. The architecture of VPON is formulated by integrating several access networks and different operators. It can provide additional services with required processing and scheduling approaches. Thus, the operational cost is effectively minimized. The proposed VPON involves resource allocation techniques, including bandwidth allocation and wavelength allocation. This allocation procedure can effectively manage the traffic load at VPON. This procedure is flexible for large scale networking environments. The proposed framework of VPON is given in Fig. 1. It includes several flexible control nodes (FCNs), ONUs, and a central management station (CMS) based on user data. CMS is the base technology of OMAN that ensures better networking with the core environment. It is located at the center of the access and base network structure. The FCN is used to control the processing of VPON.

Moreover, several other user nodes and OLTs are used to enhance the communication performance. The node consists of adjustable transceivers and wavelength connecting equipment in the ONU. All the resources are collected in OLU, and they are communicated with OLT for efficient network access. ONUs are operated across OLUs and VPONs. For each VPON, connections are permitted to allocate wavelength resources. In the VPON structure, the ONU and OLTs are controlled with FCN. Flexibility can be achieved through the virtual pattern of FCN. If the communication is required to be upgraded, then the OLT and FCN requirements are modified by the VPON. During the processing of VPON, the OLT model and the number of OLTs are not modified. This is static during the overall processing of the VPON system. Several kinds of services required by the user are handled effectively through VPON operations.

### Wavelength and bandwidth allocation with WU-DWA

#### Wavelength allocation among VPON

Before allocating bandwidth, VPONs must share available wavelengths optimally to balance load and meet demands dynamically. The efficient wavelength allocation ensures efficient resource utilization. Initially, the traffic proportion  $\delta_m$  is estimated as:

$$\delta_m = \frac{\sum_{a=1}^r (E_a + A_a + B_a)}{H \cdot \epsilon_k} \quad (1)$$

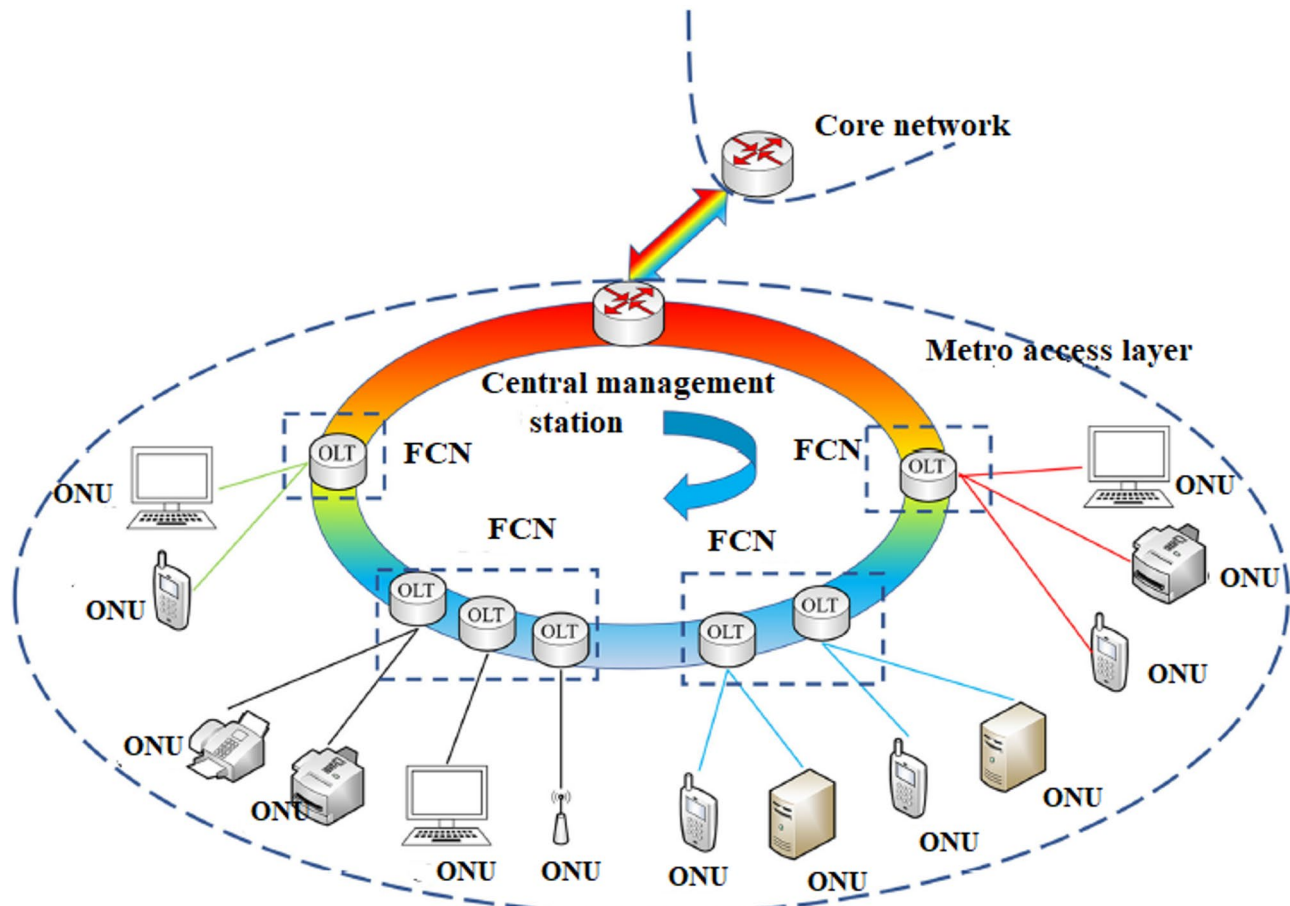


**Fig. 1.** Proposed multi-wavelength VPON architecture.

The number of ONUs is symbolized as  $r$ , the bandwidth requested by  $a^{th}$  ONU concerning the best effort, assured forwarding, and expedited forwarding is signified as  $E_a$ ,  $A_a$ , and  $B_a$  respectively. The capacity of one wavelength is signified as  $H$ , and the number of wavelengths allocated to the VPON is indicated as  $\epsilon_k$ . Initially, all the wavelengths are distributed equally among the VPON, and then the remaining wavelength is allocated to VPONs with the highest traffic demand. By considering the traffic proportion, the proportion sorting is devised to identify the high demand VPON. Then, the excess bandwidth  $D_{over,m}$  of the VPON is estimated as:

$$D_{over,m} = \sum_{a=1}^r (E_a + A_a + B_a) - H \cdot \epsilon_k. \quad (2)$$

Then, the overflow concatenation is devised and is described as:

$$D_{over} = \sum_{m=1}^G \max(D_{over,m}, 0). \quad (3)$$

Here, the total count of VPON is symbolized as  $G$ . For the dynamic re-allocation, transfer one wavelength from the VPON with the smallest  $\delta_m$  to the one with the largest  $\delta_m$ , recalculate  $D_{over}$ , and repeat until the overflow is minimized.

#### Bandwidth allocation among VPON

After determining wavelength allocations, bandwidth resources within each VPON are distributed among ONUs based on requested demands and service priority. The priority is categorized into three categories: lowest priority (best effort), medium priority (assured forwarding), and highest priority (expedited forwarding). In order to prevent starvation of lower-priority services by limiting expedited forwarding allocation, the constraint considered is:

$$\text{MaxEBandwidth} = \chi \cdot T_{BW}. \quad (4)$$

The constraint parameter  $\chi$  has the bounds of  $(0 < \chi < 1)$ . Let the total bandwidth requested be:

$$T_L = \sum_{a=1}^r E_a + A_a + B_a. \quad (5)$$

Prior to the resource allocation, the total VPON capacity  $T_{BW}$  is compared with the total requested bandwidth  $T_L$ . At first, temporary bandwidth allocation is devised and is described as:

$$D_{E,temporary}^a = L_E^a \quad (6)$$

$$D_{A,temporary}^a = L_A^a \quad (7)$$

$$D_{B,temporary}^a = L_B^a. \quad (8)$$

The temporary bandwidth allocated for best effort, assured forwarding, and expedited forwarding is notated as  $D_{B,temporary}^a$ ,  $D_{A,temporary}^a$  and  $D_{E,temporary}^a$ , respectively. The bandwidth concerning the best effort, assured forwarding, and expedited forwarding of  $a^{th}$  ONU is signified as  $L_B^a$ ,  $L_A^a$ , and  $L_E^a$  respectively. Then, the remaining energy is calculated as:

$$D_{rem} = T_{BW} - \sum_{a=1}^r L_B^a + L_A^a + L_E^a. \quad (9)$$

After estimating the remaining energy, the bandwidth allocation is devised as:

$$D_E^a = D_{E,temporary}^a + D_{E,pre}^a \quad (10)$$

$$D_A^a = D_{A,temporary}^a + D_{A,pre}^a \quad (11)$$

$$D_B^a = D_{B,temporary}^a + D_{B,pre}^a. \quad (12)$$

The predicted bandwidth for best effort, assured forwarding, and expedited forwarding is signified as  $D_{B,pre}^a$ ,  $D_{A,pre}^a$ , and  $D_{E,pre}^a$  respectively. Reallocation of bandwidth is devised iteratively until resources are fully utilized or constraints are met.

#### Data aggregation with APC traffic grooming

In data aggregation, the data is collected from several end users to enhance the network performance and better resource utilization. The key idea is to combine or groom multiple low-bandwidth data streams into higher-capacity data channels to optimize the use of available network resources, such as wavelengths in optical networks or channels in general communication systems. Data aggregation in the PON network is important since heterogeneous data collected from different users requires more energy in order to send data. The solution for minimizing the energy is to process and aggregate the data before sending. This requires the data to be aggregated before the transmission process. In the traffic grooming-based technique, the data traffic is effectively handled with high-capacity networks. It consists of organizing, reshaping or consolidating the traffic to make

the use of available resources like bandwidth. It reduces the resource consumption and reduces the overhead associated with separate connections.

The input data is considered as  $Y = [Y_1, \dots, Y_i]$  with size  $p \times i$ , where  $Y_j$  represents the  $j^{th}$  feature with size  $m \times 1$  and  $\sum Y_j = 0$ . The parameter  $Y$  is assumed to be zero centric, and the required number  $i$  leads to Eigen vectors. The following steps are used for proposed data aggregation.

Step 1: For the input data, the covariance of the data is estimated as  $\sum Y = YY^T$  and the value of  $q$  are assigned as 1. The Eigen vectors are initialized as  $\mu_q$  with size  $p \times 1$ .

Step 2: The value of  $\mu_q$  is updated using and the orthogonalization process is invoked for  $\mu_q$ . Then it is normalized by dividing it by the norm.

$$\mu_q = \mu_q - \sum_{k=1}^{q-1} (\mu_q^T \mu_k) \mu_k \quad (13)$$

$$\mu_q = \mu_q / \|\mu_q\|. \quad (14)$$

Step 3: If the value of  $\mu_q$  is not converged, then continue with step 2. In this, the basis vector converges when the new and old value points are in the same direction.

Step 4: The value of  $q$  is incremented to and then the random initialization procedure is continued until  $q = i$ .

Step 5: The orthogonal projection matrix is obtained as  $\Omega = [\mu_1, \mu_2, \dots, \mu_i]$ . Then, the columns of the projection matrix are sorted in descending order of relevant eigenvalues. Finally, the projection data is calculated as  $A = Y\mu$ .

### Routing based on adaptive tuna salp swarm optimization

Routing is based on the objective of selecting the optimal node by considering the characteristics, including energy, network lifetime, delay, and packet delivery ratio. The fitness function for the optimization process is modeled as follows.

$$F_n = x_1 \times En + x_2 \times NL + x_3 + PR + x_4 \times Dy. \quad (15)$$

where,  $En$  indicates the energy consumption,  $NL$  is the network lifetime,  $PR$  is the packet delivery ratio,  $Dy$  is the delay, and the normalization factors  $x_1, x_2, x_3$ , and  $x_4$  are in the interval between 0 and 1.

#### Salp swarm initialization

The initialization of the salp swarm is based on the tuna optimization approach. The initial population is randomly selected in the search space. The mathematical model for this process is represented as follows.

$$q_j^p = \text{rand}(UB - LB) + LB, j = 1, 2, 3, \dots, TP. \quad (16)$$

where,  $\text{rand}$  is a random number between  $[0, 1]$ ,  $UB$  represents the upper bound and  $LB$  represents the lower bound in the search space. The parameter  $TP$  indicates the total population, and  $q_j^p$  is the initialization of tuna population.

#### Spiral school feeding

Spiral foraging is the first foraging strategy of tuna schools. When tunas feed, they form spiral shapes that reach them to shallow water areas vulnerable to attack. The mathematical modelling of the spiral forage strategy is given as follows.

$$Y_j^{u+1} = \begin{cases} \begin{cases} \beta_1 \cdot (Y_{bst}^u + \beta \cdot |Y_{bst}^u - Y_j^u|) + \beta_2 \cdot Y_j^u, j = 1 \\ \beta_1 \cdot (Y_{bst}^u + \beta \cdot |Y_{bst}^u - Y_j^u|) + \beta_2 \cdot Y_{j-1}^u, j = 2, 3, \dots, TP \end{cases} \text{rand} < \frac{u}{u_{max}} \{ \\ \begin{cases} \beta_1 \cdot (Y_{rnd}^u + \beta \cdot |Y_{rnd}^u - Y_j^u|) + \beta_2 \cdot Y_j^u, j = 1 \\ \beta_1 \cdot (Y_{rnd}^u + \beta \cdot |Y_{rnd}^u - Y_j^u|) + \beta_2 \cdot Y_{j-1}^u, j = 2, 3, \dots, TP \end{cases} \text{rand} < \frac{u}{u_{max}} \{ \end{cases} \quad (17)$$

$$\beta_1 = b + (1 - b) \cdot \frac{u}{u_{max}} \quad (18)$$

$$\beta_1 = (1 - b) - (1 - b) \cdot \frac{u}{u_{max}} \quad (19)$$

$$\gamma = e^{cm} \cdot \cos(2\pi c). \quad (20)$$

$$m = e^{-3\cos(((u_{max} + 1/u - 1)\pi))} \quad (21)$$

In this equation,  $Y_j^{u+1}$  represents the position of the individual in  $u + 1$  iteration,  $Y_{bst}^u$  represents the optimal position of the current individual, the position  $Y_{rnd}^u$  is randomly generated based on an individual in the search space.  $\beta_1, \beta_2$  are the weight coefficients for controlling the movement towards optimal individual. The parameter  $d$  indicates the degree of the coefficient,  $u$  represents the number of iterations,  $u_{max}$  indicates the maximum number of iterations,  $m$  and  $\gamma$  are intermediate variables, and  $c$  is a random number. When all tunas spiral forage around a food source, they can search effectively to attain the optimal solution. The search efficiency of the optimal individual is decreased when best performing individual fails to detect the food. Similarly, the global search ability is integrated with random individual positions for spiral searching. When the number of iterations increases, the local search capability and search precision are enhanced to achieve an optimal solution.

#### Tuna parapolice foraging

Parabolic feeding is the second feeding strategy, where each tuna swims with the previous one to form parabolic shapes. Moreover, the tuna search for food around themselves and the mathematical modelling is given below.

$$Y_j^{u+1} = \begin{cases} Y_{bst}^u + rnd.(Y_{rnd}^u - Y_j^u) + T_F \cdot q^2 \cdot (Y_{rnd}^u - Y_j^u) & rnd < 0.5 \\ T_F \cdot q^2 \cdot Y_j^u \cdot rnd & \geq 0.5 \end{cases} \quad (22)$$

$$q = \left(1 - \frac{u}{u_{max}}\right)^{\left(\frac{u}{u_{max}}\right)} \quad (23)$$

where,  $T_F$  represents the random number between  $-1$  and  $1$  for controlling the population in the direction. The parameter  $q$  is the adjustment factor for controlling the magnitude of the population. Based on these two strategies, the tunas continuously updated their position until the termination criterion was reached. In each iteration, the optimal position is updated based on the fitness value.

#### Salp swarm-based position update strategy

The Salpidae family, to which the salp belongs, resembles jellyfish in both arrangement and motility. SSA is a swarm intelligence technique that makes use of the sea's dynamic salp pattern. Each salp is a member of a group known as a salp chain, in which they exhibit a swarm. Additionally, the main salp serves as the leader, while the other salps follow. Let us consider the chain of  $P$  salps moves in a bounded  $D$ -dimensional space, focusing on the optimal solution. The update rule is based on the position of the leader salp. In  $k^{th}$  dimension with  $k = 1, \dots, E$ , the update rule for the leader salp swarm is given as follows.

$$y_k^1 = \begin{cases} G_k + d_1 ((UB_k - LB_k)d_2 + LB_k) if d_3 \geq 0 \\ G_k - d_1 ((UB_k - LB_k)d_2 + LB_k) if d_3 < 0 \end{cases} \quad (24)$$

The upper and lower bounds in the  $k^{th}$  dimensional search space is represented as  $UB_k$ , and  $LB_k$  respectively. In  $k^{th}$  dimension, the position with the best solution is represented as  $G_k \in [LB_k, UB_k]$  which is related to the best food source. When increasing the number of iterations,  $d_1$  is decreased exponentially. The increase in  $d_1$  is based on the following rule.

$$d_1 = 2e^{-(\frac{4m}{M})^2}. \quad (25)$$

where,  $M$  is the total number of iterations, and  $m$  is the current iteration. Finally, both  $d_2$  and  $d_3$  are the random numbers uniformly selected in the range of  $[0, 1]$ . The major issue related to SSO is the variants with respect to  $G_k$  which is given as,

$$d_1 ((UB_k - LB_k)d_2 + LB_k) = d_1 d_2 (UB_k - LB_k) + d_1 LB_k. \quad (26)$$

The value of  $[0, UB_k - LB_k]$  is given by  $d_1 d_2 (UB_k - LB_k)$ , the value of  $d_1 LB_k$  added, and this value is a large arbitrary value. In the SSO search process, the large constant is shifted in the search space. In a  $D$ -dimensional space, if  $LB_k = 10^l$  and  $UB_k = 10^l + 1$  with  $k = 1, \dots, E$ . Also, the search space is a hypercube  $[10^l, 10^l + 1]^k$ . Based on the updated rule, the leader salp is modified as follows.

$$y_k^1 = G_k \pm d_1 d_2 (UB_k - LB_k) + d_1 LB_k \quad (27)$$

$$y_k^1 = G_k \pm d_1 d_2 + d_1 10^l. \quad (28)$$

The related locations are updated based on the following expression.

$$y_k^n = \frac{1}{2}(y_k^n - y_k^{n-1}). \quad (29)$$

where,  $n \geq 2$ , and  $y_k^n$  indicates the position of  $n^{th}$  affiliate at  $k^{th}$  dimension. The algorithm for the SSO approach is given as follows.

## Algorithm 1: Salp swarm algorithm

Input: The total population is considered as nodes
Output: The Best position is selected as the optimal node
1. Initialize population using the Tuna optimization algorithm
2. For each iteration
3. do
4. Estimate each salp of population
5. Detect best salp as $G_k$
6. Update $y_k$ by eqn. 2.
7. For each salp $y_k$
8. do
9. if $y_k$ is the leader then
10. Update location with eqn. 1
11. else
12. Update the location by eqn. 6
13. return f
14. end

**Experimental evaluation**

The proposed energy efficient OAN is simulated in MATLAB, and the performance is evaluated with standard performance metrics. Also, the performance of the proposed approach is compared with existing state-of-the-art approaches. The performance of the proposed approach is compared with existing approaches, including Association Rule-Based Routing Protocol (ARBRP), Event-Based Routing (EBR), Distance based Routing (DBR) and Social Relationship-based Energy Efficient Routing (SEER) approaches.

The simulation parameters used are given in Table 2.

The number of active OLT transceivers is computed with different traffic loads as shown in Fig. 2, and values are given in Table 3. When increasing the traffic load from 0.1 to 1, the OLT transceiver utilization increases. For 0.6 traffic overload, the number of active OLT transceivers is 14.1, 14, 13, 10, and 7 for EBR, DBR, ARBRP, SEER, and the Proposed approach. When varying the traffic load, the alive OLT transceivers are varied as 4, 7, 14, and 18 for the proposed approach. The results indicate that the proposed approach has a low OLT transceiver, which indicates better wavelength efficiency. In the case of existing approaches, the performance is poor due to inactive components in the network architecture.

The minimal cover radius of the proposed approach is compared with existing approaches by considering different traffic loads in Fig. 3; Table 4. The traffic load of the proposed approach varies from 0.1 to 1, and the performance is noted. The minimal cover radius obtained with the proposed approach is 40.51, 45.06, and 48.6 for the traffic load 0.6, 0.8, and 0.9. Also, the minimal cover radius varies from 127.72, 114.07, 70.34, 55.67, and 48.6 for EBR, DBR, ARBRP, SEER, and the proposed approach. This cover radius is based on the shortest link

Simulation Parameter	Value
Number of VPON	4
Number of OLT	1
Number of available wavelengths	16
Number of ONU	64 (each VPON)
Packet size	64-1518 bytes
Packet distribution	Uniform
Data rate	0-10 Mbps
Data generation rate	0-100 Mbps
Data generation	Random
Transmission rate	1Gbps
Guard time slot	1 $\mu$ s

**Table 2.** Simulation parameters.

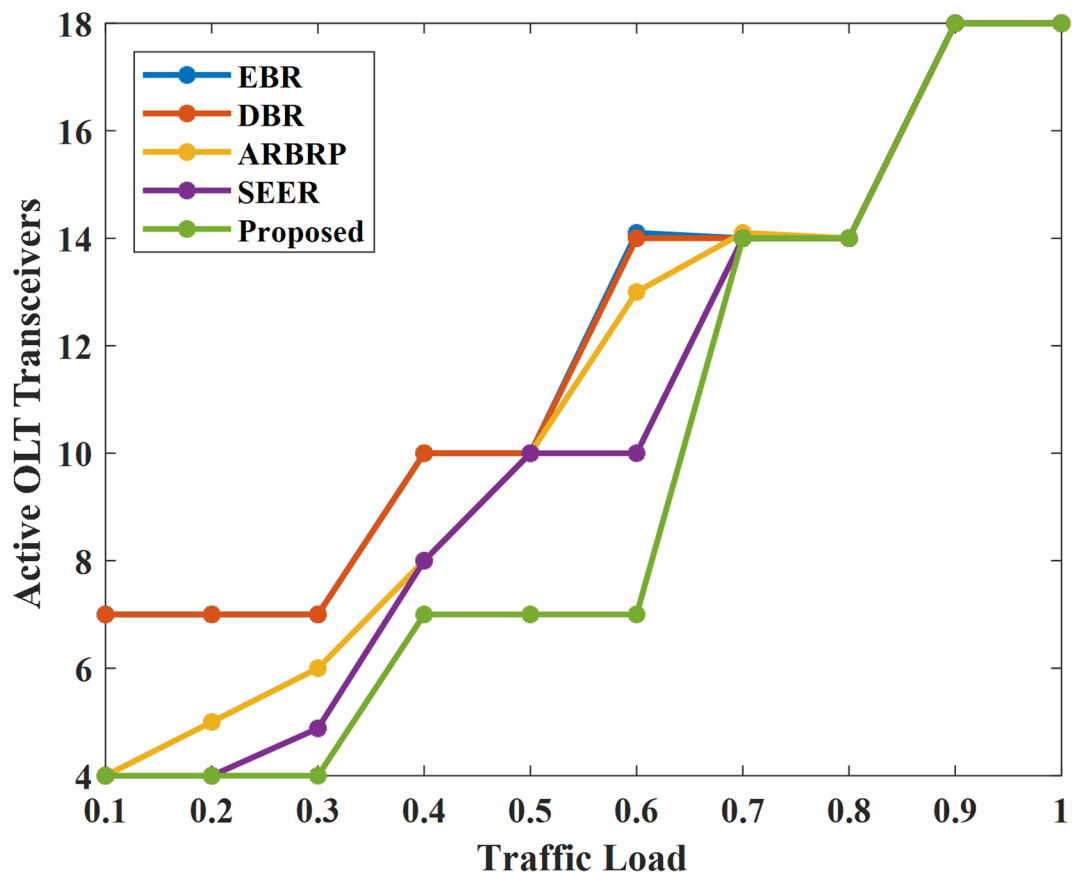


**Fig. 2.** The number of active OLT transceivers vs. traffic load.

Traffic Load	Active OLT Transceivers				
	EBR	DBR	ARBRP	SEER	Proposed
0.1	7	7	4	4	4
0.2	7	7	5	4	4
0.3	7	7	6	5	4
0.4	10	10	8	8	7
0.5	10	10	10	10	7
0.6	14.1	14	13	10	7
0.7	14	14	14.1	14	14
0.8	14	14	14	14	14
0.9	18	18	18	18	18
1	18	18	18	18	18

**Table 3.** Number of active OLT transceivers with varying traffic load.

used for the transmission. If the link is interconnected, then the access reach of the link is computed with the length of the feeder link and the node distribution length. Initially, the small network radius is achieved, and the traffic load is increased. In the same scenario, the minimal cover radius indicates poor performance. The minimal cover radius of the proposed approach indicates better performance, which is obtained with the highest traffic load.

The maximum access radius of the proposed approach is compared with existing approaches by varying the traffic load in Fig. 4; Table 5. This rate is measured based on the maximum available reach of the transmission link. It is noted that the proposed approach can ensure better access than existing approaches. When the traffic load increases, the maximum access reach of all approaches is increased. This performance is due to the traversing nature of the ONU-OLT transmission link, and it can be enhanced with the proposed routing approach. The maximum access radius of the proposed approach is varied to 224.931, 211.07, 208.61, 208.09, 202.92, 194.63,

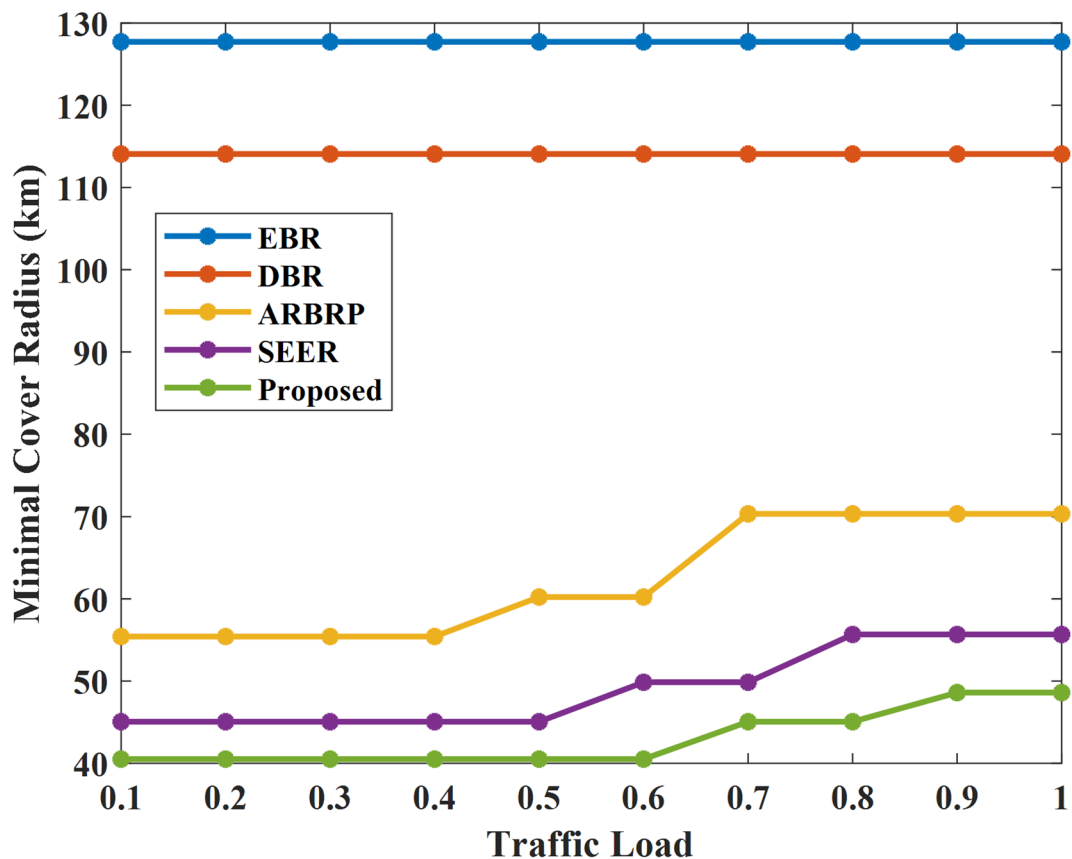


**Fig. 3.** The minimal cover radius vs. traffic load.

Traffic load	EBR	DBR	ARBRP	EBR	Proposed
0.1	127.72	114.07	55.42	26.77	40.51
0.2	127.72	114.07	55.42	26.77	40.51
0.3	127.72	114.07	55.42	26.77	40.51
0.4	127.72	114.07	55.42	26.77	40.51
0.5	127.72	114.07	60.22	33.17	40.51
0.6	127.72	114.07	60.22	33.17	40.51
0.7	127.72	114.07	70.34	46.66333	45.06
0.8	127.72	114.07	70.34	46.66333	45.06
0.9	127.72	114.07	70.34	46.66333	48.6
1	127.72	114.07	70.34	55.67	48.6

**Table 4.** Minimal cover radius performance with varying traffic load.

185.52, 175.58, 175.05, and 172.03 for the proposed approach. The maximum access radius is 115.28, 134.81, 145.1, 155.13, and 172.032 for EBR, DBR, ARBRP, SEER, and the Proposed approach.

The average packet delivery ratio of the proposed approach by varying traffic overload, is given in Fig. 5 and Table 6. When the traffic load increases, the average packet delay increases. Average packet delay for the proposed approach varies as 3.551, 4.798, 5.177, 5.42, 5.565, 5.652, 5.768, 5.923, 6.039, and 6.272 for the proposed approach. In the case of EBR, DBR, ARBRP, SEER, and Proposed approaches, the delay varies to 7.461, 7.344, 7.246, 6.603, and 6.272, respectively. This delay is lower for the proposed approach and higher for the existing approaches. The packet delay increased the number of hops between the source and destination. This delay is increased due to processing, queuing, transmission, etc (Table 6).

The energy savings of the proposed approach are estimated by varying the traffic load from 0.1 to 1 in Fig. 6, Table 7. In the proposed routing approach, the forwarder node is selected based on energy efficiency. The total energy saved by EBR, DBR, ARBRP, SEER, and Proposed approaches is 20.261, 21.87, 23.523, 28.565, and 29.998 with the traffic load of 1. Moreover, the energy saved with the proposed approach is varied to 25.348, 25.534, 25.808, 26.475, 26.926, 27.636, 27.868, 28.708, 29.245, and 29.998 for different traffic loads. Hence, the proposed

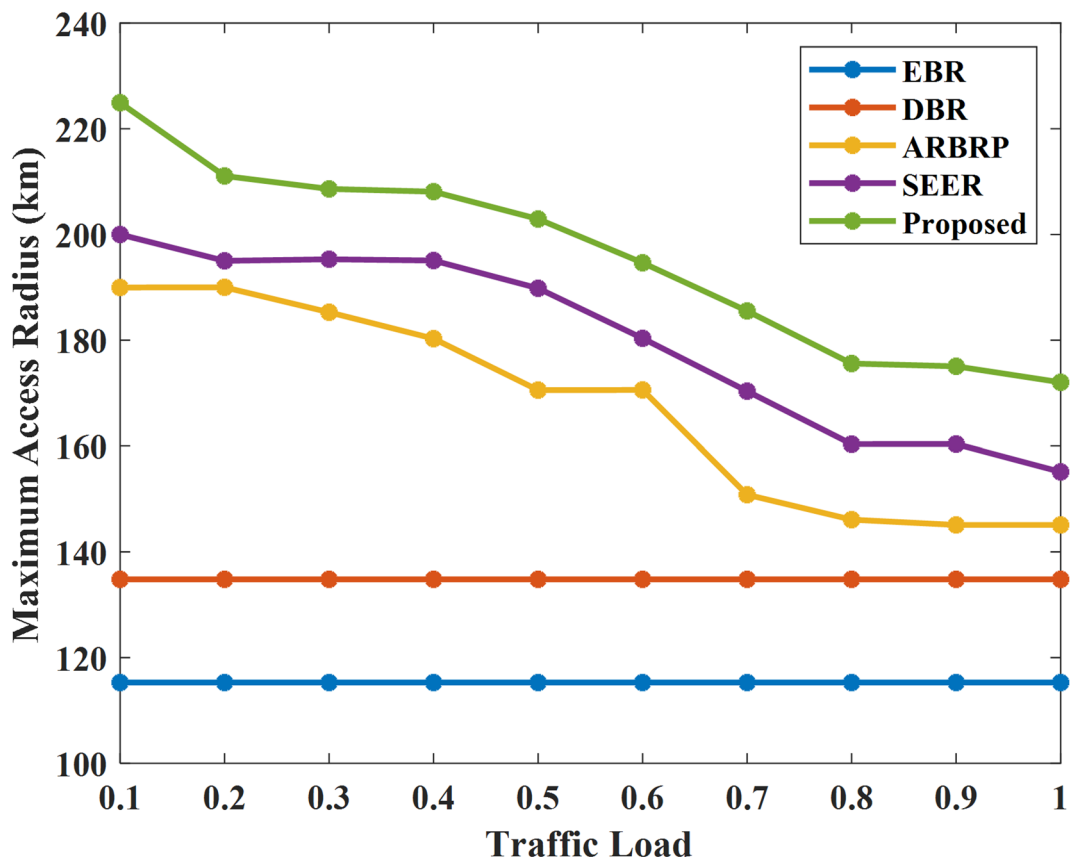


**Fig. 4.** Maximum access radius vs. traffic load.

Traffic load	EBR	DBR	ARBRP	SEER	Proposed
0.1	115.28	134.81	189.97	200	224.931
0.2	115.28	134.81	190	195.01	211.0721
0.3	115.28	134.81	185.28	195.31	208.614
0.4	115.28	134.81	180.29	195.07	208.0995
0.5	115.28	134.81	170.55	189.82	202.923
0.6	115.28	134.81	170.58	180.35	194.6385
0.7	115.28	134.81	150.82	170.35	185.5245
0.8	115.28	134.81	146.1	160.35	175.581
0.9	115.28	134.81	145.1	160.38	175.056
1	115.28	134.81	145.1	155.13	172.032

**Table 5.** Maximum access radius performance with varying traffic load.

model improves energy efficiency. When traffic load increases, energy efficiency increases. For the proposed approach, the energy efficiency is higher than that of existing approaches. Lower energy savings are achieved for existing approaches.

The energy consumption performance by varying the number of nodes is given in Fig. 7; Table 8. The number of nodes varies from 3 to 9, and the energy consumption is evaluated. When the number of nodes increases, the energy consumption increases. The energy consumption is slightly deviated up to 5 nodes. After that, the deviation is higher, and the performance is severely affected. However, the highest energy consumption achieved was 210 for the proposed approach. In the case of existing approaches, the energy consumption level is increased to 310. The higher energy consumption is due to the ineffective data transmission process of existing techniques.

The energy consumption of the proposed approach with varying transmission probability is given in Fig. 8; Table 9. The transmission probability varies from 0.1 to 0.9. When the transmission probability increases, the energy consumption increases. When varying the transmission probability to 0.3, the energy consumption gradually increases and then slightly increases. Only a slight deviation is noted from 0.3 to 0.9, which indicates that the transmission probability is not affected after 0.3. In the case of existing approaches, the energy consumption

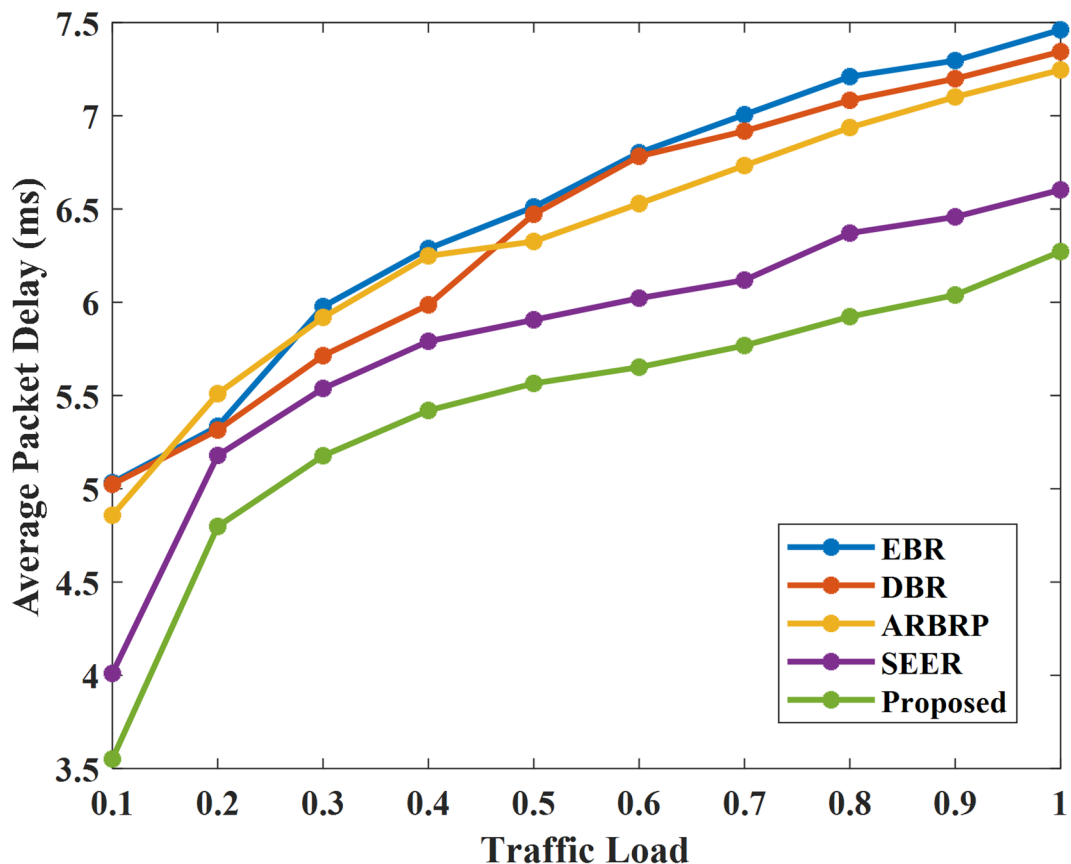


**Fig. 5.** Average packet delay vs. traffic load.

Traffic load	EBR	DBR	ARBRP	SEER	Proposed
0.1	5.033	5.024	4.858	4.01	3.551
0.2	5.335	5.315	5.51	5.179	4.798
0.3	5.977	5.714	5.919	5.538	5.177
0.4	6.288	5.986	6.249	5.791	5.42
0.5	6.511	6.472	6.326	5.906	5.565
0.6	6.802	6.783	6.529	6.022	5.652
0.7	7.006	6.918	6.733	6.119	5.768
0.8	7.21	7.083	6.937	6.371	5.923
0.9	7.296	7.199	7.101	6.458	6.039
1	7.461	7.344	7.246	6.603	6.272

**Table 6.** Average packet delay performance with varying traffic load.

is linearly increased based on the transmission probability. The lower energy consumption of 90 is obtained for the proposed approach and 160 for the existing SEER approach with a 0.1 transmission probability. Furthermore, the energy consumption reaches 200 for a 0.9 transmission probability of the proposed approach. The energy consumption of the proposed approach is higher than the energy consumption of existing approaches. Lower energy consumption of the proposed approach is due to the efficient routing paradigm, which is based on an optimal energy strategy.

For the proposed framework, network lifetime is estimated by varying transmission probability in Fig. 9; Table 10. The transmission probability varies from 0.1 to 0.9. When the transmission probability increases, the network lifetime is reduced. A higher transmission network lifetime of the proposed approach is achieved with the transmission probability of 0.1. The lifetime performance of EBR, DBR, ARBRP, SEER, and the proposed approach is 210849.00, 303624.78, 366266.01, 400000.71, and 489162.05 for 0.1 transmission probability. Moreover, the lifetime of the proposed approach is higher than the lifetime of existing approaches in all transmission probabilities. The higher lifetime is due to lower power consumption.

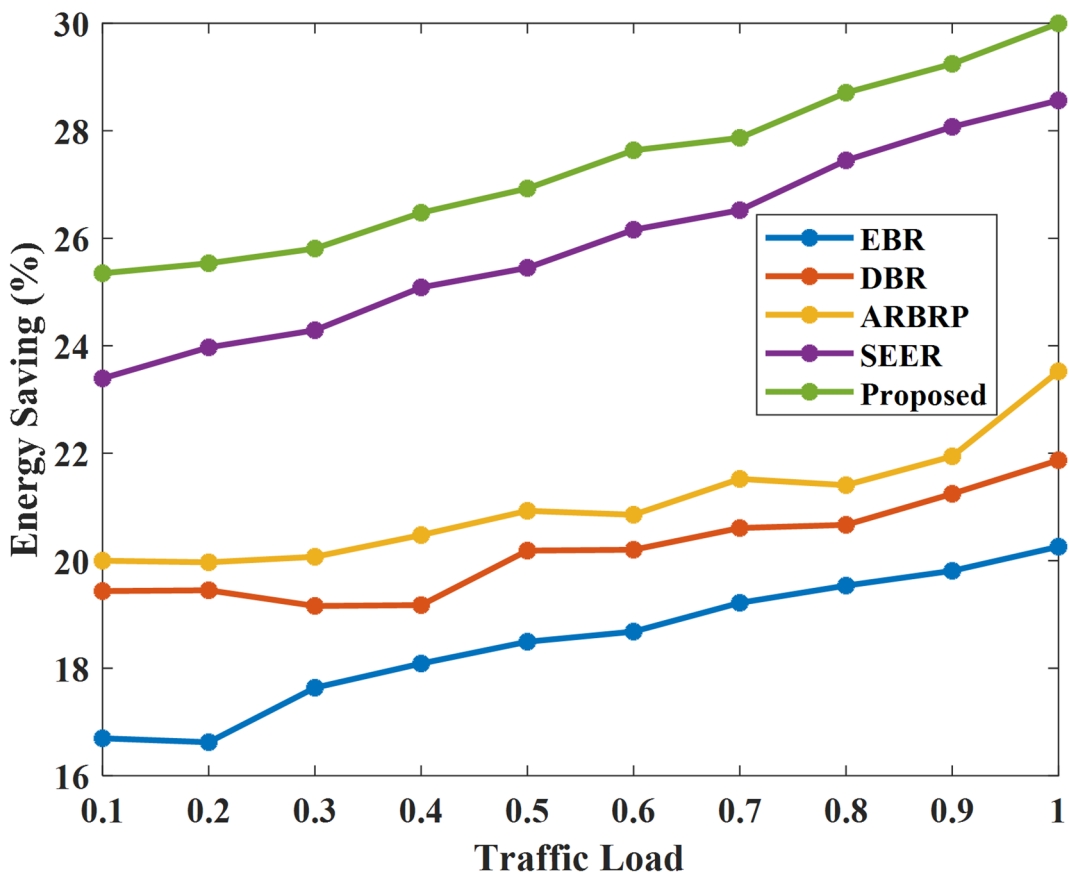


**Fig. 6.** Energy savings vs. traffic load.

Traffic load	EBR	DBR	ARBRP	SEER	Proposed
0.1	16.696	19.435	20	23.392	25.348
0.2	16.623	19.45	19.971	23.97	25.534
0.3	17.637	19.158	20.073	24.289	25.808
0.4	18.087	19.174	20.477	25.085	26.475
0.5	18.493	20.188	20.928	25.45	26.926
0.6	18.681	20.204	20.855	26.158	27.636
0.7	19.217	20.609	21.522	26.522	27.868
0.8	19.537	20.667	21.406	27.449	28.708
0.9	19.812	21.245	21.942	28.073	29.245
1	20.261	21.87	23.523	28.565	29.998

**Table 7.** Estimated energy savings with varying traffic load.

Figure 10; Table 11 show the throughput performance of the suggested method when the number of nodes is changed. The number of nodes varies from 20 to 110, and the performance is evaluated. When the number of nodes increases, the throughput also increases. When varying the number of nodes to 20, 40, 60, 80, and 100, the proposed throughput varies to 131.63, 160.30, 282.20, 313.87, and 361.60, respectively. Also, the throughput performance obtained with EBR, DBR, ARBRP, SEER, and the proposed approach is 125.02, 70.15, 245.32, 316.49, and 361.60 for 100 nodes. The throughput performance obtained with the proposed approach is higher than the throughput of existing approaches. The higher throughput is due to the proposed paradigm's efficient routing techniques. When considering the performance of all metrics, higher performance is obtained with the proposed approach. This indicates that the proposed optical access network is energy efficient and highly preferable.

The proposed Energy Efficient Regional Area MOAN introduces a novel architecture for high-capacity metropolitan optical networks, with a focus on minimizing energy consumption and maximizing throughput and efficiency. The system integrates WU-DWA, APCA based traffic data aggregation, and ATSSO based energy aware routing. WU-DWA dynamically assigns wavelengths based on real-time utility metrics, ensuring efficient

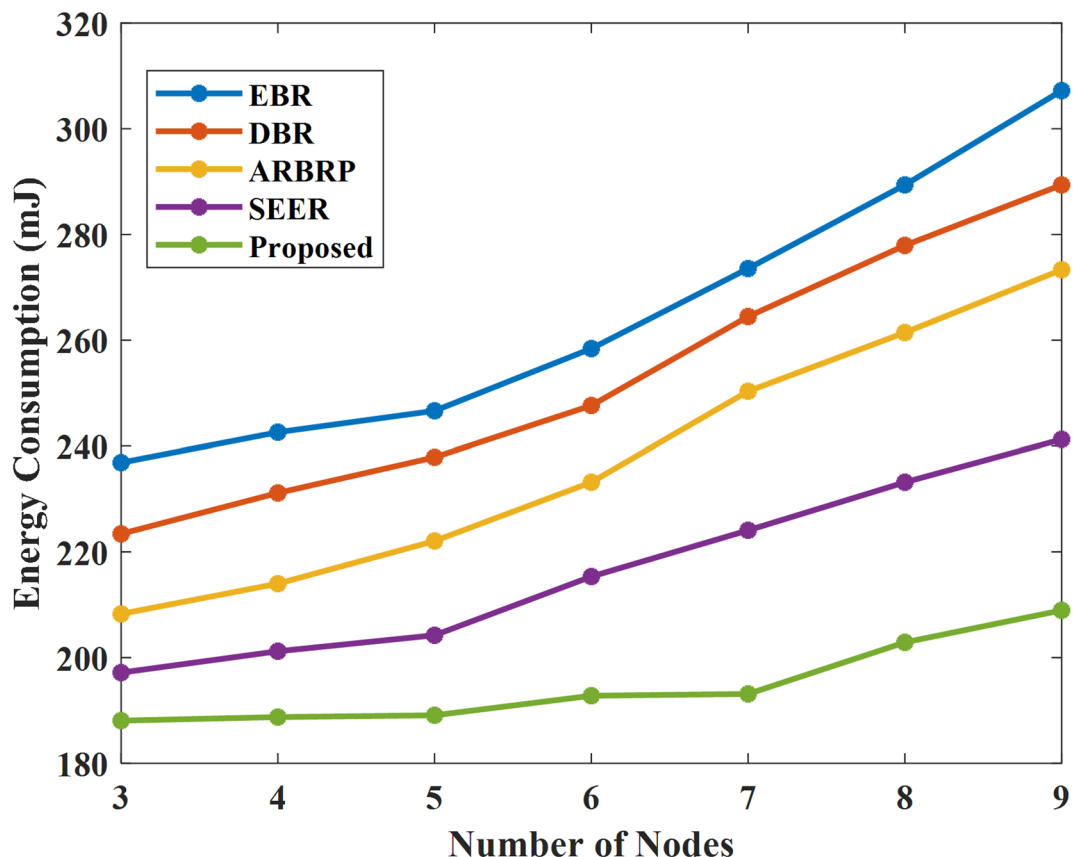


**Fig. 7.** Energy consumption vs. number of nodes.

No. of nodes	Energy Consumption (mJ)				
	EBR	DBR	ARBRP	SEER	Proposed
3	236.875	223.4135	208.2692	197.1635	188.07692
4	242.5962	231.1539	213.9904	201.2019	188.75
5	246.6346	237.8846	222.0673	204.2308	189.08654
6	258.4135	247.6442	233.1731	215.3365	192.78846
7	273.5577	264.4712	250.3365	224.0865	193.125
8	289.375	277.9327	261.4423	233.1731	202.88462
9	307.2115	289.375	273.3173	241.25	208.94231

**Table 8.** Energy consumption performance with varying number of nodes.

resource utilization. Unlike static allocation, WU-DWA reduces idle capacity and enables better balancing of optical bandwidth, which directly contributes to improved throughput (131.63) and reduced energy waste in underutilized channels.

The use of APCA for traffic grooming allows the system to identify correlations among data flows and combine them intelligently into fewer high-capacity streams. This minimizes redundant transmissions and optical switching operations, which significantly reduces total energy consumption (88 units) and improves network efficiency. By reducing the number of active optical elements needed for routing, APCA also contributes to a lower average packet delay (3.551 ms). ATSSO is a metaheuristic algorithm that adapts to network conditions by selecting routing paths that optimize energy cost functions while maintaining performance constraints. Compared to traditional algorithms (like Dijkstra or ACO), ATSSO better explores the search space and avoids local minima by simulating adaptive foraging behavior of tuna swarms. This leads to a measurable energy saving of 29.99%, showing that the routing paths selected consume significantly less power while still meeting quality-of-service requirements.

Traditional systems often use static or heuristic-based wavelength allocation, which leads to underutilized channels and poor resource optimization. In contrast, WU-DWA adapts in real time, improving spectral efficiency. Existing traffic aggregation techniques may not leverage the underlying statistical properties of traffic.

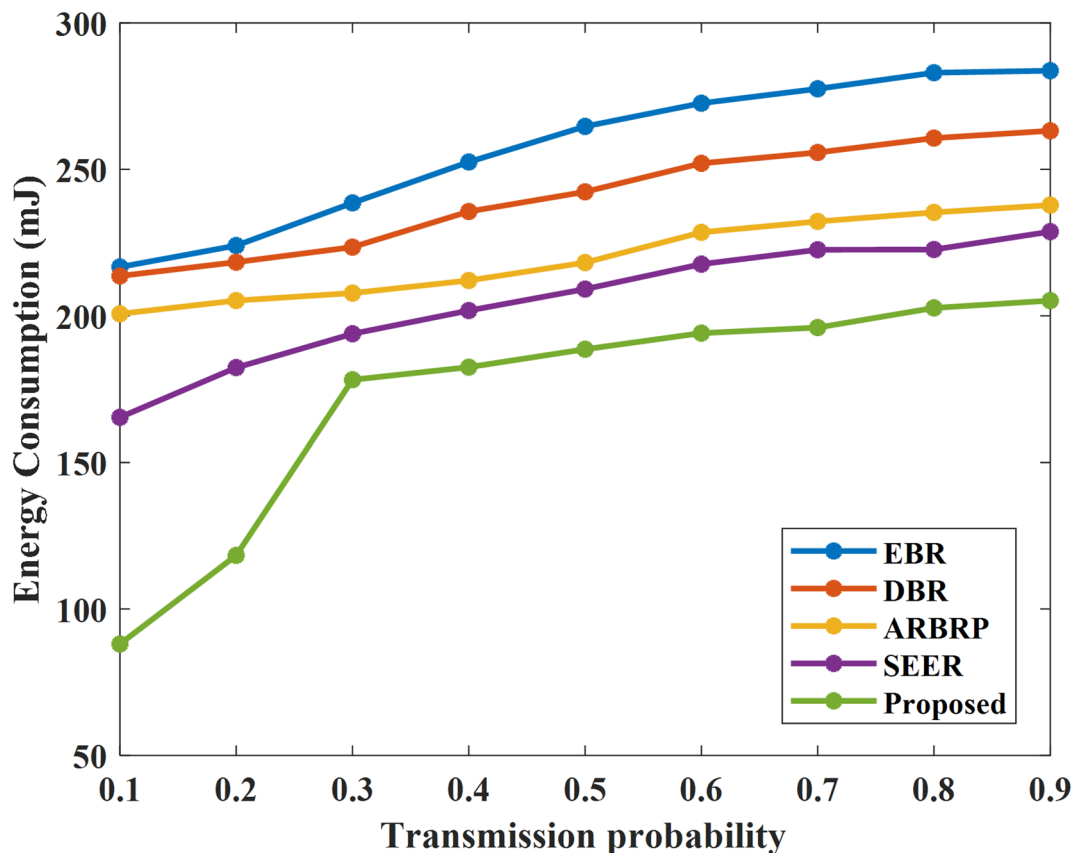


**Fig. 8.** Energy consumption vs. transmission probability.

Transmission probability	Energy Consumption (mJ)				
	EBR	DBR	ARBRP	SEER	Proposed
0.1	216.6685	213.6105	200.6803	165.3435	88.04527
0.2	223.9874	218.3256	205.2123	182.3225	118.31735
0.3	238.5581	223.4606	207.7619	193.873	178.16895
0.4	252.5214	235.614	212.0651	201.7985	182.47395
0.5	264.6721	242.3354	218.1781	209.1264	188.58875
0.6	272.6012	252.0698	228.5173	217.6504	194.09789
0.7	277.5083	255.7718	232.2229	222.5602	195.98654
0.8	283.0183	260.6771	235.3157	222.631	202.70252
0.9	283.6957	263.1678	237.8037	228.7422	205.19413

**Table 9.** Energy consumption performance with varying transmission probability.

By using APCA, the system adapts to temporal and spatial patterns, reducing overhead and unnecessary data duplication. Many energy-aware routing protocols do not balance global energy cost with local traffic behavior. ATSSO's bio-inspired approach allows for globally optimal, yet traffic-aware path selection, making it superior in dynamic, large-scale scenarios. The combined effect of dynamic allocation, statistical grooming, and intelligent routing creates synergy across layers of the network, rather than optimizing only a single function. This end-to-end co-optimization is the key reason for outperforming prior models in all measured metrics.

## Conclusion

The development of OMAN relies heavily on VPON because of their capacity to effectively manage resources and support a variety of services. In this paper, energy-efficient traffic data aggregation and energy-aware routing are developed for VPON. Traffic data aggregation reduces redundant transmissions, while energy-aware routing minimizes energy consumption by selecting energy-efficient paths. These strategies can help balance network performance with sustainability goals. The combination of energy-aware routing, dynamic wavelength and bandwidth allocation, and traffic data aggregation can significantly improve energy efficiency in Metro-

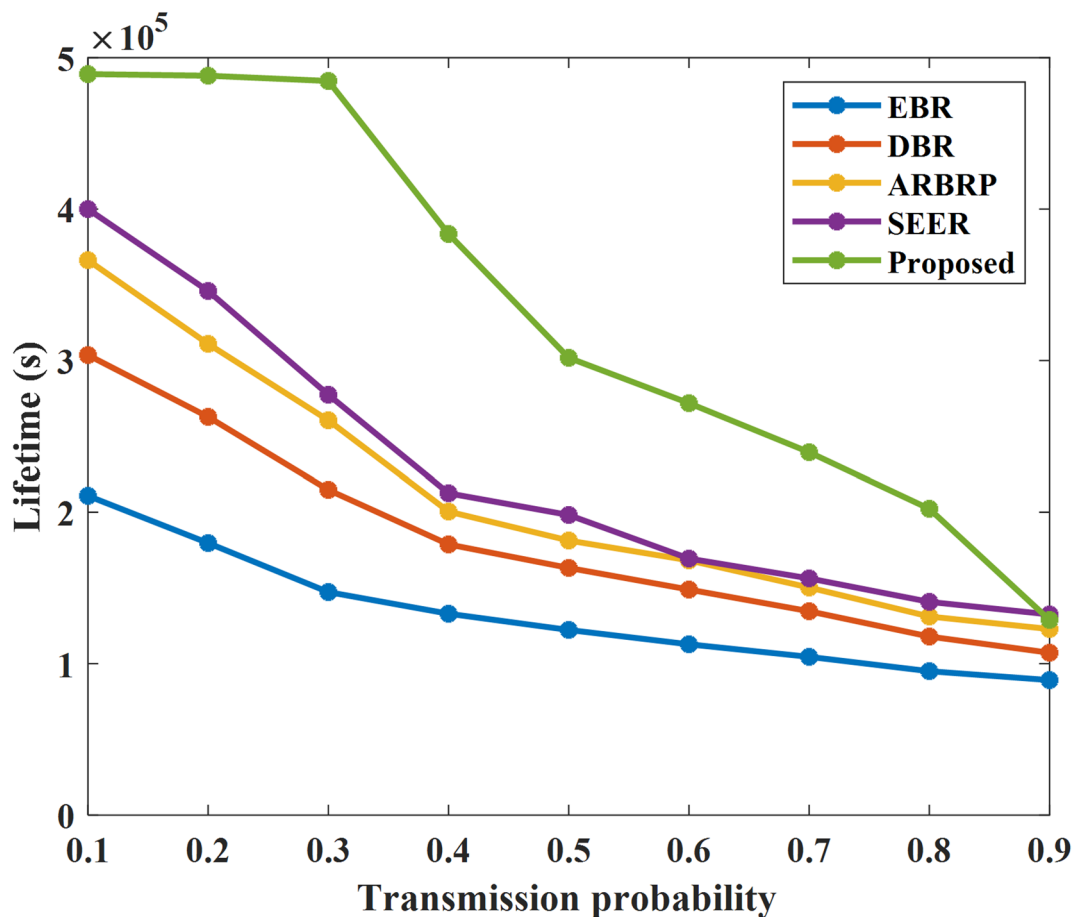


**Fig. 9.** Lifetime vs. transmission probability.

Transmission probabilities	EBR	DBR	ARBRP	SEER	Proposed
0.1	210,849	303624.8	366,266	400000.7	489162.1
0.2	179659.6	262796.9	310992.9	345,927	488101.8
0.3	147293.9	214754.4	260537.2	277409.9	484635.5
0.4	132989.7	178767.1	200469.8	212505.4	383581.4
0.5	122289.2	163259.9	181339.2	198199.4	301,806
0.6	112802.4	148955.7	168,238	169435.6	271839.2
0.7	104525.8	134640.7	150308.6	156334.4	239,461
0.8	95046.18	117923.3	131,178	140830.8	202254.7
0.9	89161.34	107233.5	122892.5	132534.5	128,913

**Table 10.** Network lifetime performance with varying transmission probability.

Access Optical Networks. Moreover, the performance of the proposed approach is evaluated and compared with existing approaches. The energy consumption, throughput, average packet delay, and energy savings obtained with the proposed approach are 188, 131.63, 3.551, and 29.99, respectively. In addition to that, the energy savings of EBR, DBR, ARBRP, SEER, and the proposed approach are 16.696, 19.435, 20, 23.392, and 25.348, respectively. These methods ensure that the network dynamically adapts to real-time conditions while maintaining high performance and low energy consumption. The proposed approach can be extended to 6G optical front haul focusing on enhancing network flexibility, improving data transmission capacity, enhancing energy efficiency, and reducing latency. Therefore, a coherent optical access communication network is suggested as a promising technology for improving efficiency, performance, and capacity of optical front haul networks for 6G networks. By considering 6G optical front haul, future research should prioritize energy efficient modulation techniques, advanced materials, and innovative transceiver architecture for reducing power consumption while maintaining performance standards. Moreover, dynamic resource allocation approaches with the integration of AI and

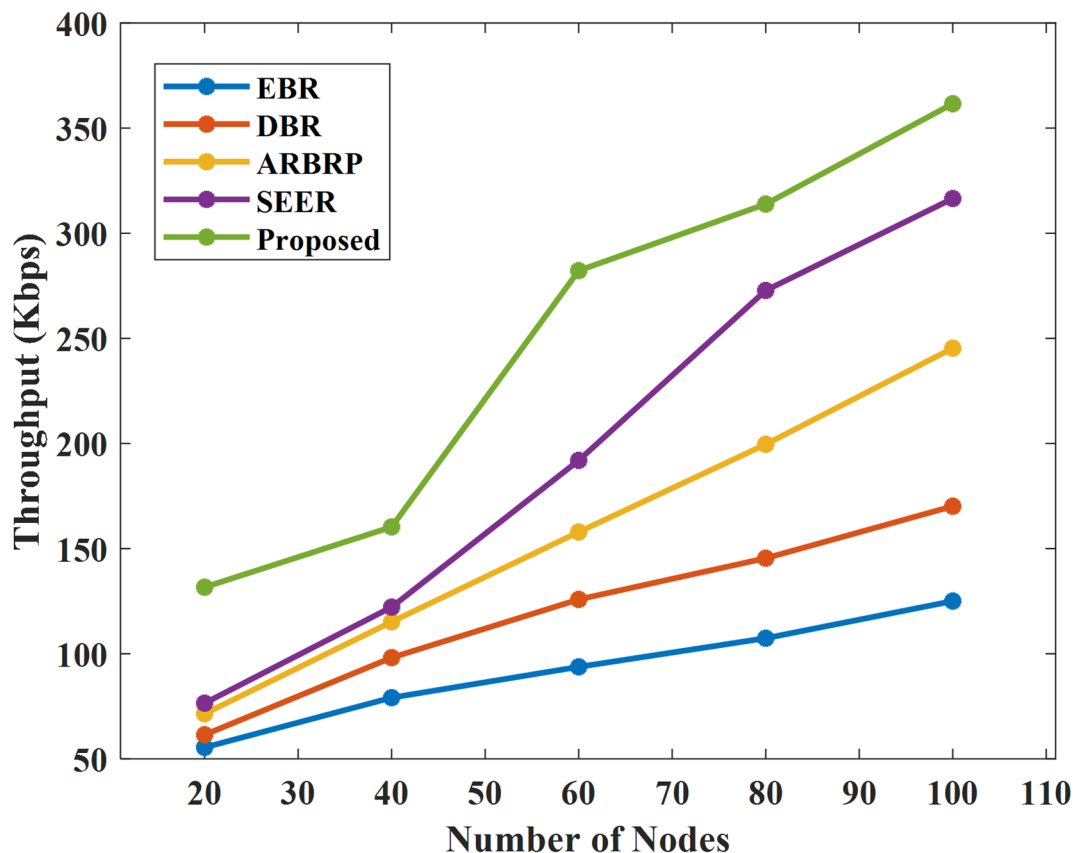


**Fig. 10.** Throughput vs. Number of nodes.

No.of nodes	Throughput (Kbps)				
	EBR	DBR	ARBRP	SEER	Proposed
20	55.44298	61.44659	71.46564	76.48355	131.6359
40	79.09778	98.13901	115.1641	122.1814	160.3086
60	93.74718	125.8149	157.8881	191.9551	282.2049
80	107.3773	145.4263	199.5929	272.7839	313.8794
100	125.0229	170.1506	245.3242	316.4992	361.6045

**Table 11.** Throughput performance with varying number of nodes.

ML techniques can adjust to varying channel conditions and traffic load, improving optimized and predictive resource utilization for energy efficient operations.

### Data availability

The data(s) used to support this study is provided within this Manuscript.

Received: 5 March 2025; Accepted: 6 June 2025

Published online: 01 October 2025

### References

1. Ullah, R. et al. A high-capacity optical metro access network: Efficiently recovering fiber failures with robust switching and centralized optical line terminal. *Sensors* **24** (4), 1074 (2024).
2. Luo, Y. & Effenberger, F. What is beyond 50G: Future standards of optical access networks. *J. Opt. Commun. Netw.* **16** (7), C106–C112 (2024).
3. Eltraify, A. E. A., Mohamed, S. H., Jaafar, M. H. & Elmirghani VM placement over WDM-TDM AWGR PON based data centre architecture. In *22nd International Conference on Transparent Optical Networks (ICTON)*, pp. 1–5. IEEE, 2020., pp. 1–5. IEEE, 2020. (2020).
4. Zhou, J. et al. KeshuangZheng et al. Flexible coherent optical access: architectures, algorithms, and demonstrations. *Journal Lightwave Technology* (2024).

5. Sachdeva, S., Shukla, M. K., Sindhwan, M., Kumar, A. & Adhikari, M. S. Comparative analysis of techniques in long reach passive optical networks: overview and design. *J. Opt. Commun.* **45** (s1), s2327–s2331 (2025).
6. Senthil Kumar, T., Mohan, V. & Senthilkumar, S. Energy efficient transmission using optical access network: Issues and challenges. *Int. J. Eng. Sci. Technol.* **7** (1), 43–51 (2023).
7. Senthil Kumar, T. V. Mohan Energy efficient regional area metropolitan optical access network (RAMOAN) using modified load adaptive sequence arrangement (LASA). *Methodol. Int. Trans. Electr. Energy Syst.*, **23**, (2023).
8. Alqahtani, A. M. et al. Energy Efficient VM Placement in a Heterogeneous Fog Computing Architecture. *arXiv preprint arXiv:2203.14178* (2022).
9. Biswas, P., Akhtar, M. S., Saha, S., Majhi, S. & Adhya, A. Q-learning-based energy-efficient network planning in IP-over-EON. *IEEE Trans. Netw. Serv. Manage.* **20** (1), 3–13 (2022).
10. El-Nahal, F., Xu, T., AlQahtani, D. & Leeson, M. A bidirectional WDM-PON free space optical (FSO) system for fronthaul 5 G C-RAN networks. *IEEE Photonics J.* **15** (1), 1–10 (2023).
11. Konstantinou, D. et al. Bart smolders, and Idelfonso Tafur monroy. 5G RAN architecture based on analog radio-over-fiber fronthaul over UDWDM-PON and phased array fed reflector antennas. *Opt. Commun.* **454**, 124464 (2020).
12. Butt, R., Aslam, M., Faheem, M., Waqar Ashraf, AsadArfeen, K. A. M. & Khawaja, A. Sleep-aware wavelength and bandwidth assignment scheme for TWDM PON. *Opt. Quant. Electron.* **53** (6), 295 (2021).
13. Tiang, J. et al. An efficient algorithm for resource optimization in TWDM passive optical network using a C-RAN. *Front. Phys.* **12**, 1429750 (2024).
14. Nsafoa-Yeboah, K., Tchao, E. T., Kommay, B. & SelasiAgbemenu, A. Griffith selormklogo, and Nana Kwadwo Akrasi-Mensah. Flexible open network operating system architecture for implementing higher scalability using disaggregated software-defined optical networking. *IET Networks.* **13** (3), 221–240 (2024).
15. AbbasianDehkordi, S., Farajzadeh, K., JavadRezazadeh, R., Farahbakhsh, K. S. & MasihAbbasianDehkordi A survey on data aggregation techniques in IoT sensor networks. *Wireless Netw.* **26** (2), 1243–1263 (2020).
16. Hall, M., Nance, K. T., Foerster, S., Schmid & RamakrishnanDurairajan A survey of reconfigurable optical networks. *Opt. Switch. Netw.* **41**, 100621 (2021).
17. Kaszubowska-Anandarajah, A. et al. Reconfigurable photonic integrated transmitter for metro-access networks. *J. Opt. Commun. Netw.* **15** (3), A92–A102 (2023).
18. Araújo, I., Brizido, A. & Lima, S. R. Virtual network function development for NG-PON access network architecture. *J. Netw. Syst. Manage.* **31** (4), 78 (2023).
19. Calvo-Salcedo, A. F., Guerrero, N., González, Jose, A. & Jaramillo-Villegas Dynamic spectrum assignment in passive optical networks based on optical integrated microring resonators using machine learning and a routing, modulation level, and spectrum assignment method. *Appl. Sci.* **13** (24), 13294 (2023).
20. Ganesan, Elaiyasuriyan, I-S., Hwang, A. T., Liem & SyuhaimiAb-Rahman, M. 5G-enabled tactile internet resource provision via software-defined optical access networks (SDOANs). In *Photonics*, vol. 8, no. 5, 140. MDPI, (2021).
21. Xu, D. et al. Dynamic hierarchical reinforcement learning framework for Energy-Efficient 5G base stations in urban environments. *IEEE Trans. Mob. Comput.* (2025).
22. Escobedo, F. & Canales, H. B. G. Fernando Willy Morillo Galarza, Carlos Miguel Aguilar Saldaña, Eddy Miguel Aguirre Reyes, and César Augusto Flores Tananta. Energy Efficient Business Management System for Improving QoS in Network Model.
23. Alhazmi, A. S. et al. Access-Point to Access-Point Connectivity for PON-based OWC Spine and Leaf Data Centre Architecture. *arXiv preprint arXiv:2404.14143* (2024).
24. Fadlelmula, Wafaa, B. M. et al. Energy Efficient Resource Allocation for Demand Intensive Applications in a VLC Based Fog Architecture. In *23rd International Conference on Transparent Optical Networks (ICTON)*, pp. 1–6. IEEE, 2023., pp. 1–6. IEEE, 2023. (2023).
25. Pakpahan, A. F. & Hwang, I-S. Peer-to-Peer federated learning on Software-Defined optical access network. *IEEE Access* (2024).
26. Garg, S. & Dixit, A. Evaluating power saving techniques in passive optical access networks. *Photon Netw. Commun.* **42**, 1–14 (2021).
27. Alharthi, M., Mohamed, S. H., Taisir El-Gorashi, E. H. & JaafarElmirghani, M. H. Resilience in PON-based data centre architectures with two-tier cascaded AWGRs. In *24th International Conference on Transparent Optical Networks (ICTON)*, pp. 1–6. IEEE, 2024., pp. 1–6. IEEE, 2024. (2024).
28. Le, G. et al. Reliable provisioning with degraded service using multipath routing from multiple data centers in optical metro networks. *IEEE Trans. Netw. Serv. Manage.* **20** (3), 3334–3347 (2023).
29. Hosseini, S., de Miguel, I. & de la Merayo, R. M. Noemí Lorenzo, and Ramón J. Durán Barroso. Energy efficient multipath routing in space division multiplexed elastic optical networks. *Computer Networks* **244** : 110349. (2024).
30. Wang, Y. et al. Security-aware 5G RAN slice mapping with tiered isolation in physical-layer secured metro-aggregation elastic optical networks using heuristic-assisted DRL. *J. Opt. Commun. Netw.* **15** (12), 969–984 (2023).

## Author contributions

All the authors contributed to this research work in terms of concept creation, conduct of the research work, and manuscript preparation.

## Declarations

### Competing interests

The authors declare no competing interests.

### Additional information

**Correspondence** and requests for materials should be addressed to T.S.K.

**Reprints and permissions information** is available at [www.nature.com/reprints](http://www.nature.com/reprints).

**Publisher's note** Springer Nature remains neutral with regard to jurisdictional claims in published maps and institutional affiliations.

**Open Access** This article is licensed under a Creative Commons Attribution-NonCommercial-NoDerivatives 4.0 International License, which permits any non-commercial use, sharing, distribution and reproduction in any medium or format, as long as you give appropriate credit to the original author(s) and the source, provide a link to the Creative Commons licence, and indicate if you modified the licensed material. You do not have permission under this licence to share adapted material derived from this article or parts of it. The images or other third party material in this article are included in the article's Creative Commons licence, unless indicated otherwise in a credit line to the material. If material is not included in the article's Creative Commons licence and your intended use is not permitted by statutory regulation or exceeds the permitted use, you will need to obtain permission directly from the copyright holder. To view a copy of this licence, visit <http://creativecommons.org/licenses/by-nc-nd/4.0/>.

© The Author(s) 2025